A two-dimensional experimental-numerical approach to investigate wave transformation over muddy beds

**Mohsen Soltanpour · S. Abbas Haghshenas ·
Tomoya Shibayama**

Abstract The effect of a thin fluid mud layer on nearshore
two-dimensional wave transformation is studied through nu-
merical modeling and wave basin experiments. The wave
basin experiments were conducted on both muddy and fixed
beds. A mixture of commercial kaolinite and tap water was
used as fluid mud layer, where its rheological viscoelastic
parameters were derived from rheometer cyclic tests. The
results can be utilized for better understanding of the complex
wave transformation phenomena under real field conditions
where the combined effects of shoaling, refraction, and dif-
fraction as well as wave energy dissipation due to existing
mud beds and wave breaking jointly occur. A dissipation
model was coupled to the combined refraction and diffraction
1 (*REF/DIF* 1) wave model to develop a numerical wave
height transformation model for muddy beaches. The pro-
posed model was utilized to analyze the experimental data
on muddy beds. Comparing the computed values of wave

heights over mud layer with the corresponding measurements
shows a fair agreement.

1 Introduction

A prerequisite for the reliable estimation of waves on maritime
structures is a detailed understanding of how waves transform
during their propagation (Goda 2000). Considerable decay of
wave energy over muddy beds along the wave trajectory may
take place over short spatial scales, i.e., a few wave lengths.
This makes wave transformation in such cases quite different
compared with sandy environments. There are many phenom-
ena contributing to coastal processes in muddy environments.
Wave attenuation as well as mud mass transport in the fluid
mud layer has been widely studied in different ways during
the past decades (e.g., Gade 1958; Dalrymple and Liu 1978;
Isobe et al. 1992; Rodriguez and Mehta 2001; Sheremet et al.
2005; Winterwerp et al. 2007). The role of soft mud to
dissipate waves has been investigated through laboratory ex-
periments by many researchers (e.g., Sakakiyama and Bijker
1989; Ross and Mehta 1990; Shibayama and An 1993; de
Boer et al. 2009; Samsami and Soltanpour 2011; Hsu et al.
2013). However, the past laboratory experiments of wave–
mud interaction are mostly on horizontal beds and consider
cross-shore direction only. The relative shortage of wave basin
research facilities, in comparison to wave flumes, the difficul-
ties of dealing with large quantity of mud, and the mobility of
fluid mud on slopes might be responsible for the lack of
comprehensive laboratory investigations on two-dimensional
wave transformation over fluid mud beds in the literature.
Soltanpour et al. (2008) presented four wave basin runs of

M. Soltanpour
Civil Engineering Department, K. N. Toosi University of
Technology, No. 1346, Vali-Asr St., Tehran 1996715433, Iran
e-mail: soltanpour@kntu.ac.ir
URL: http://wp.kntu.ac.ir/soltanpour/

S. A. Haghshenas (✉)
Institute of Geophysics, University of Tehran, North Kargar Ave.,
P.O. Box 14155-6466, Tehran 1439551113, Iran
e-mail: sahaghshenas@ut.ac.ir
URL: http://geophysics.ut.ac.ir/faculty/sahaghshenas

T. Shibayama
Waseda University, Tokyo, Japan
e-mail: shibayama@waseda.jp
URL: http://www.f.waseda.jp/shibayama/

wave transformation over a small mud section measured 1 m by 1 m. However, their results were affected by the small size of mud section.

An extensive variety of studies have been conducted for simulating wave energy dissipation by a nonrigid muddy bed. Since Gade (1958) who initiated the study on the behavior of cohesive bed materials under wave action by assuming a viscous fluid model, different constitutive equations have been assumed for prediction of the response of muddy beds. Assuming viscous rheological behavior of fluid mud, Dalrymple and Liu (1978) developed a two-layer mud–water system to evaluate wave attenuation. Tsuruya et al. (1987) proposed a multi-layered viscous fluid system to analyze the interaction between surface water waves and a mud bed. Ng (2000) used the assumption of a thin mud layer to propose a simplified numerical approach of the Dalrymple and Liu (1978) model.

Based on a set of data from field studies in the Gulf of Mexico, Sheremet and Stone (2003) proposed a theory regarding the possible role of wave–wave interactions in mediating short-wave dissipation. Their numerical simulations suggest that nonlinear energy transfer within the wave spectrum may be important, providing the necessary coupling between the short-wave and long-wave spectral bands and, thereby, causing energy to transfer to long waves, where it can be efficiently dissipated via direct wave–bottom interaction. The effect of a thin viscous fluid–mud layer on near-shore nonlinear wave–wave interactions is studied by Kaihatu et al. (2007). They employed a parabolic frequency–domain nonlinear wave model, assuming a bottom dissipation mechanism based on a viscous boundary layer approach. Although the complex two-dimensional wave propagation was successfully simulated, the mud rheology and the dissipation rate were simplified by assuming simple viscous behavior of fluid mud and Ng (2000) relations, respectively. Next, also the rheological assumption of a viscoelastic fluid (e.g., Macpherson 1980; Maa 1986; Maa and Mehta 1988; Jain and Mehta 2009), a Bingham plastic medium (e.g., Mei and Liu 1987; Sakakiyama and Bijker 1989), or a viscoelastic-plastic behavior (Shibayama and An 1993) has been made to describe the behavior of fluid mud at the seafloor.

Modeling of wave damping at Guyana mud coast was performed by Winterwerp et al. (2007). Wave damping by mud was simulated through a modification of simulating waves nearshore (SWAN) based on an extension by De Wit (1995) of the Gade (1958) formulation. They employed small-scale wave attenuation laboratory experiments as well as measurements reported by Wells and Kemp (1986). A favorable agreement was obtained between model results and applied data from wave height measurements. Recently, Kranenburg et al. (2011) presented the so-called SWAN–mud model, which is an extension to the SWAN wave model, in order to simulate wave damping in coastal areas by soft

mud deposits through the implementation of a new dispersion relation and energy-dissipation equation obtained from a viscous two-layer model schematization.

The aim of the present study was to extend the results of the laboratory experiments to a better understanding of two-dimensional wave propagation over muddy beds for developing and applying numerical model simulations. Therefore, the present study offers a large set of wave basin experiments on a general three-dimensional bathymetry under regular monochromatic waves in order to investigate the wave transformation over mud layers. Adopting perpendicular and oblique incident waves, the experiments were conducted on both muddy and fixed beds to obtain comparable results with and without mud presence. Next, the combined refraction and diffraction 1 (REF/DIF 1) wave model is employed and modified to develop a two-dimensional wave transformation model including the dissipative effects of the nonrigid bed (Kirby and Dalrymple 1983). Defining a two-dimensional domain for the wave transformation model and assuming viscoelastic rheological equations for fluid mud behavior, a multi-layered fluid system is employed to compute the wave attenuation rate. The viscoelastic parameters of fluid mud are derived from the rheological laboratory experiments. The calculated values of the energy dissipation rates in the study area are introduced to the REF/DIF 1 wave transformation model to simulate wave propagation. The results from the wave basin experiments have been utilized in the two-dimensional extended REF/DIF 1 wave model for better understanding of the complex wave transformation phenomena under real conditions where the combined effects of shoaling, refraction, and diffraction as well as wave energy dissipation due to mud bed existence and wave breaking are present.

The setup of this paper starts with describing details of the experimental investigation in Section 2, and thereafter, the obtained data from the laboratory tests are analyzed and some primary conclusions are made in Section 3. Section 4 describes the details of the numerical model proposed for simulating wave propagation over a muddy bed. Section 5 assesses the model performance against laboratory data and discusses the findings of the study. Summarizing the study, the final conclusions are presented in Section 6.

2 Laboratory experiments

2.1 Experimental setup

Two-dimensional wave basin experiments were carried out at the hydraulic laboratory of Yokohama National University. The basin was measured 10.5 m (length) by 9.0 m (width) with a bottom slope of 1:30. Figure 1 shows the top view of the wave basin.

Fig. 1 A top view of the experimental setup

Commercial kaolinite was used to prepare the fluid mud bed because of its similar rheological behavior with natural mud and also due to its reproducible properties and easy handling. The distribution of particle sizes of the used kaolinite follows the point $D_{86}=10$ μm. The chemical composition of kaolinite is listed in Table 1. The mud was prepared by mixing kaolinite with tap water and was put in a horizontal box in the wave basin measuring 2.7 m in both directions and 10 cm in height. Tap water was used to fill the wave basin. An iron plate with mild slopes of 1:3 to 1:2 was put on the front edge of mud box to mitigate effects of a sudden disturbing vertical change in the bottom level. Figure 2 shows the sketch of experimental setup. Fine gravel was employed in the three other sides with a slope of 1:2 to 1:4. A 1:4 slope of gravel material was also put at the end of the wave basin to reduce the amount of reflected waves.

Note that since fluid mud is not stable on a sloping bed, the designed setup differs from prototype muddy profiles. It has been considered to minimize the difference between the horizontal muddy bed and the sloping bed floor by lowering half

Table 1 Chemical composition of applied kaolinite

Composition	Percentage (%)
SiO_2	45.90
Al_2O_3	37.80
Fe_2O_3	0.60
CaO	0.01
MgO	0.04
K_2O	0.46
Na_2O	0.02
TiO_2	0.22
IgLoss	13.80

of the mud box. However, this would considerably damage the basin floor. Therefore, it was decided to put the whole mud box on the basin floor.

Monochromatic waves with different combinations of wave height and wave period were generated by the wave paddles at the edge of the basin. The upwave characteristics of waves approaching the mud section, as well as the waves at five points over the mud box, were recorded using six electric capacitance-type wave gauges. The wave measuring stations S1 to S6 are depicted in Fig. 2, where S1 stands for the upwave station and S2 to S6 show the location of wave stations over the mud patch.

The runs under monochromatic wave conditions were repeated on a fixed bed as well to provide the necessary data for comparison with wave dissipation on a muddy bed. To provide a fixed horizontal bed with the same elevation as the mud bed, the mud box was filled by concrete blocks and the small spaces between the blocks were filled by cement mortar to provide a uniform surface.

2.2 Fluid mud rheology

Rheological properties of mud samples were investigated using an Anton Paar Physica MCR300 instrument in the Rheometery Laboratory of Institute for Colorants, Paint and Coatings (ICPC) in Iran. Since the oscillatory movement better resembles mud behavior under wave action, the parameters were determined under oscillatory loading. The oscillatory frequency sweep (FS) tests were conducted to measure the viscoelastic characteristics of natural mud with different water content ratios, ranging from 110 to 160 %. Figure 3 shows the obtained results from rheometry experiments for a sample with water content ratio of 121 % where $G'=G$ is the

Fig. 2 Experimental setup sketch. S1 to S6 stand for wave measuring stations, where electric capacitance wave gauges were deployed

BASIN AND SETUP PLAN
UNITS: CM

BASIN AND SETUP SECTION
UNITS: CM
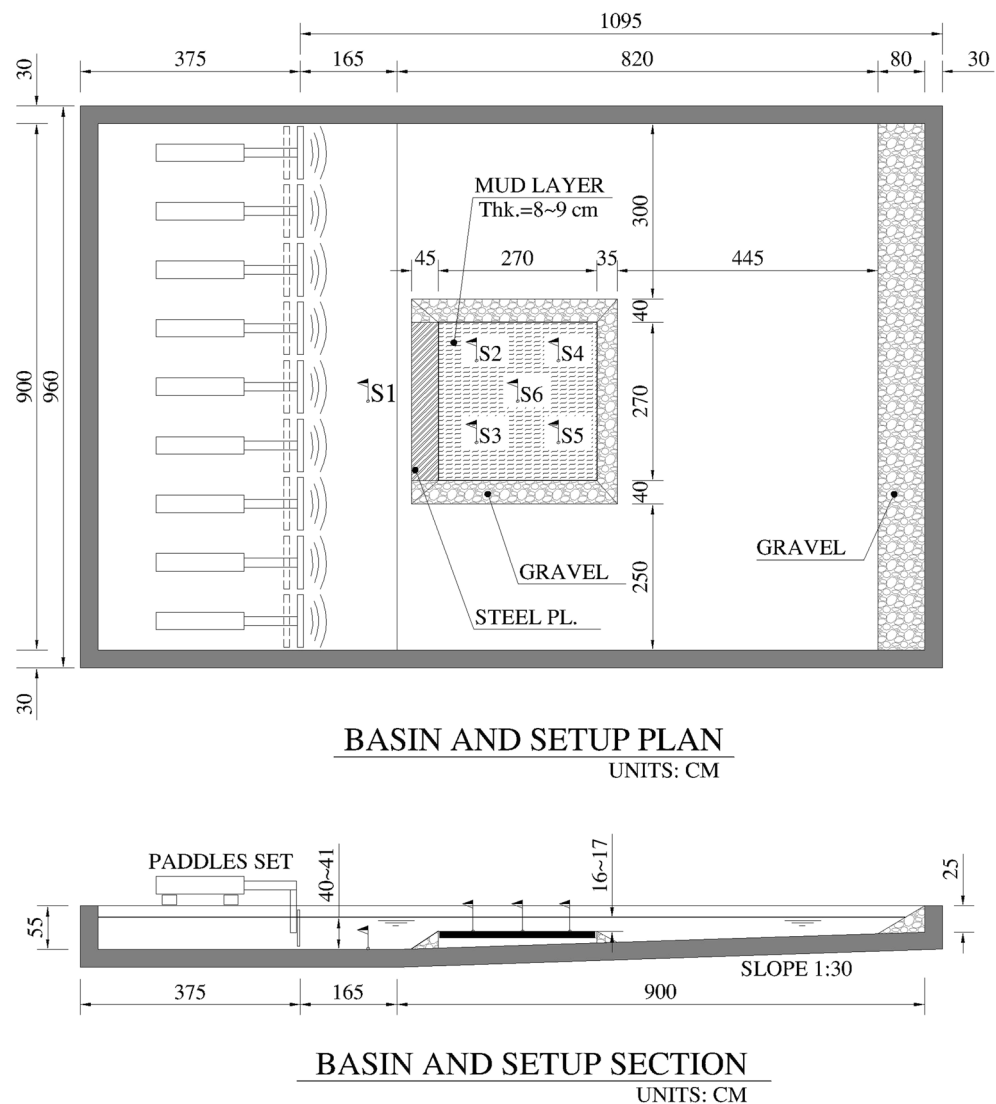
in-phase elastic or storage modulus and $G''=\mu\omega$ is the quadrature or loss modulus.

Figure 4 shows that the viscoelastic parameters of mud samples highly depend on the oscillatory period, i.e., the viscosity coefficient μ increases by increasing the oscillatory period, while the shear modulus G decreases. The relations between the viscoelastic parameters and the wave period for fluid mud with different water content ratios are presented in Table 2.

2.3 Experimental conditions

The horizontal pre-prepared kaolinite bed was subjected to constant wave action at a water depth of 16 to 18 cm over the mud surface for a duration of 5 min. The test was repeated with different combinations of wave heights, wave periods, wave angles, and water content ratios of kaolinite under monochromatic wave conditions. The selected water contents of all cases are higher than the liquid limit of kaolinite mud, which is conceptually defined as the water content at which

the behavior of mud changes from plastic to liquid. Table 3 summarizes the test conditions of seven runs with different wave characteristics, water depths, mud properties, and wave angles. Similarly, Table 4 lists relevant conditions of seven runs of wave transformation over the fixed bed for which a test duration of 5 min was adopted as well. It was not possible to generate exactly the same incident waves. However, the differences of upwave heights in the cases of mud presence and fixed bed are less than 0.7 cm.

3 Data analysis

Details of laboratory measurements and the analysis of obtained wave data are presented and discussed here. Figures 5, 6, and 7 present the results of three selected experimental cases. In each figure, the upper graph shows the wave height measurements at five stations over the mud bed and the lower

Fig. 3 Rheometry curve for storage modulus and loss modulus versus angular frequency
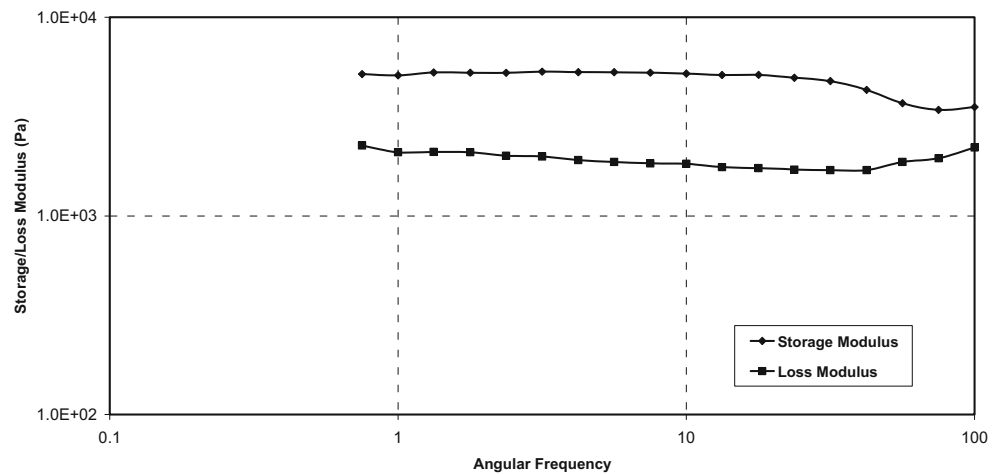

one presents the data on the fixed bed. The differences of initial wave conditions can be neglected, as described in the previous section.

The observed pattern of wave transformation is complicated mainly because of the role of different factors contributing to wave height changes. These include shoaling and diffraction as well as dissipation due to mud existence. As observed in the figures, the wave height decreases from stations 2 and 3 to station 6 and then it increases again at stations 4 and 5, although there is an exception for case FB_CS66. In the case of transforming waves over the mud bed, the decrease in wave height between stations 2 and 3 to 6 can be related to the dissipation role of mud layer. Moreover, the wave height in the beginning of the mud box can be higher than the incident wave height because of shoaling effects. The wave diffraction also results in a long-shore transfer of wave energy toward the

mud box. It should also be noted that the dissipating role of the mud bed may not be very effective near the walls of mud box compared to the middle parts of the box as observed by other researches (Shen 1993; Soltanpour et al. 2003). In the first two cases with higher frequencies, the differences between wave heights over the muddy bed and fixed bed are more significant, which might be attributed to the higher weight of mud-induced energy dissipation relative to other processes in these cases. For the third case with lower frequency, the wave heights over the box for both muddy and fixed beds are quite of the same magnitude and based on visual observations during the experiments, it seems that there is no significant energy transfer from the sides toward the mud box.

A mathematical model of the near-shore wave field was developed to determine the compound effects of shoaling, diffraction, and energy dissipation by the mud layer. The
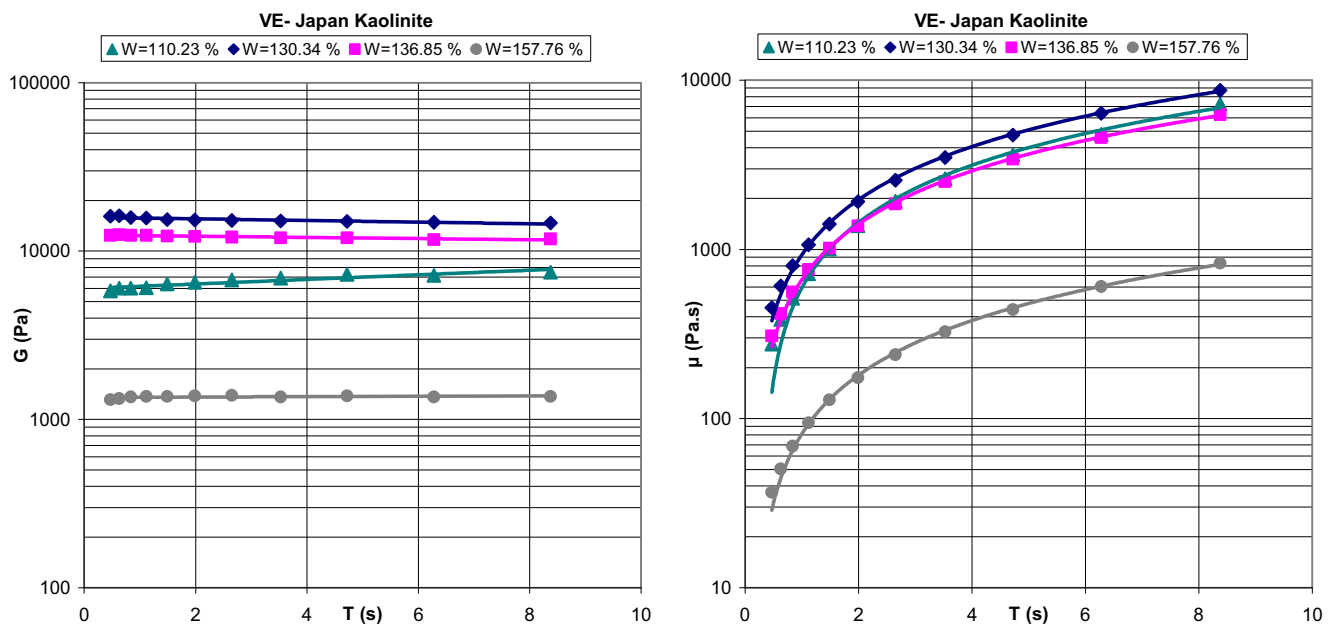
Fig. 4 Measured Kelvin–Voigt viscoelastic rheological parameters for the applied kaolinite. Elastic modulus (G) in the *left panel* and dynamic viscosity (μ) in the *right* one

Table 2 Viscoelastic parameters versus oscillatory period for different water content ratios

	W (%)	G (Pa)	μ (Pa s)
1	110.23	$5986.8\,e^{0.0314T}$	$850.98T–258.77$
2	130.34	$15{,}898\,e^{-0.0113T}$	$1040.7T–112.75$
3	136.85	$12{,}447\,e^{-0.008T}$	$749.81T–88.453$
4	157.76	$1351.8\,e^{0.0025T}$	$99.504T–18.281$

W: water content of the mud mixture, i.e., the ratio of water mass to sediment mass

outputs of the numerical model for different scenarios as well as the comparisons between the numerical model results and the obtained data for different cases are presented in the following sections.

4 Wave transformation model

The REF/DIF 1 wave model (Kirby and Dalrymple 1983), which is a so-called phase-resolving parabolic refraction-diffraction model for ocean surface wave propagation, is employed in the present study to simulate wave propagation over the physical model domain. Assuming viscoelastic rheological behavior for the artificial fluid mud, a multi-layered fluid system is employed to simulate the wave attenuation. The viscoelastic parameters of fluid mud are derived from independent rheological tests conducted on mud samples of different water contents, as presented in Section 2.2. The calculated values of the energy dissipation rates in the area covered by fluid mud are finally introduced to the REF/DIF 1 wave transformation model to simulate wave propagation over the wave basin.

4.1 REF/DIF 1 wave model

REF/DIF 1 is a weakly nonlinear combined refraction-diffraction model initially developed by Kirby and Dalrymple (1983). The model has been designed based on a Stokes expansion of water wave theory, including third-order correction to the phase speed of the waves; however, it is not a complete third-order theory, as not all third-order terms are taken into account. Applying the theory to real cases requires the application of parabolic estimations which leads to some limitations in model applicability for wave propagation directions ±60° off the assumed wave direction. The governing equation of the REF/DIF 1 wave models is a parabolic mild slope equation including a simple energy loss proposed by Dalrymple et al. (1984). The linear form of the mild slope equation with dissipation term is (Kirby and Dalrymple 1986)

$$A_x - i(k-k_0)A + \left(1\big/2C_g\right)C_{gx}A - \left(i\big/2C_g\sigma\right)\left(CC_gA_y\right)_y + \left(w\big/2C_g\right)A = 0 \tag{1}$$

where k_0 is a reference wave number given by the initial conditions of the wave field and A is a complex amplitude related to the water surface displacement through

$$\eta = Ae^{i(kx-\sigma t)} \tag{2}$$

The last term of the governing equation (1) represents wave energy dissipation in the wave model. The dissipation factor w is the energy dissipation divided by the energy with the unit of 1 over time. This factor is given by a number of different expressions, through which bottom friction losses due to rough, porous, or viscous bottoms and wave breaking or other dissipation mechanisms can be accounted for. In this study, the dissipation factor consists of two major terms, i.e., dissipation due to wave breaking and dissipation associated with the soft muddy bottom. The dissipation due to wave breaking is simulated following Kirby and Dalrymple (1986), which is an extension of the breaking model of Dally et al. (1985). The expression defining the dissipation parameter for wave breaking w_b is given as

$$w_b = \frac{KC_g\left[1-\left(\frac{\gamma h}{H}\right)^2\right]}{h} \tag{3}$$

where K and γ are coefficients determined to be equal to 0.017 and 0.4, respectively (Dally et al. 1985). Parameter H is the wave height and is equal to $2|A|$. The w_b term becomes active when breaking is supposed to take place, namely at $H > 0.78h$ in the REF/DIF model.

Table 3 Selected test conditions for wave transformation on mud layer

Run case	Wave period (s)	Incident wave height station 1 (cm)	Wave angle (deg)	Over mud water depth (cm)	Mud thickness (cm)	w (%)
MB_CS16	1.5	6.5	0.0	17.00	9.00	110
MB_CS17	1.2	8.8	0.0	17.00	9.00	110
MB_CS18	1.4	7.3	0.0	17.00	9.00	110
MB_CS19	1.8	3.9	0.0	17.00	9.00	110
MB_CS20	2.0	2.3	0.0	17.00	9.00	110
MB_CS26	1.4	6.5	−20.0	18.00	8.50	112
MB_CS29	1.2	7.0	−20.0	17.00	8.50	115

Table 4 Selected test conditions for wave transformation on fixed bed

Run case	Wave period (s)	Incident wave height station 1 (cm)	Wave angle (deg)	Over the box water depth (cm)
FB_CS61	1.5	6.5	0.0	17.00
FB_CS63	1.2	8.5	0.0	17.00
FB_CS64	1.4	7.3	0.0	17.00
FB_CS66	1.8	3.3	0.0	17.00
FB_CS59	2.0	2.0	0.0	17.00
FB_CS76	1.4	7.2	−20.0	17.00
FB_CS79	1.2	6.5	−20.0	17.00

Regarding the energy dissipation induced by the muddy bottom, a parameter w_m is adopted from results of the wave–

mud interaction model (next sub-section). The sequences of computing this parameter and introducing it to REF/DIF 1 model are discussed in the following section.

The governing equation is conveniently solved in finite difference form through the Crank–Nicolson technique. As offshore boundary condition, the incident wave is prescribed at the furthest seaward grid row, which has a constant depth. For lateral boundary conditions, a totally reflecting condition is generally used for each side.

4.2 Wave dissipation by the nonrigid soft muddy bed

For simulating wave–fluid mud interaction and calculating the wave attenuation rate, the fluid system, including the fluid mud and water layers, is divided into N sub-layers, in which

Fig. 5 Measured wave heights over the muddy bed (*up*; MB-CS17, incident wave height 8.8 cm and wave period 1.2 s) as well as the fixed bed (*down*; FB-CS63, incident wave height 8.5 cm and wave period 1.2 s)
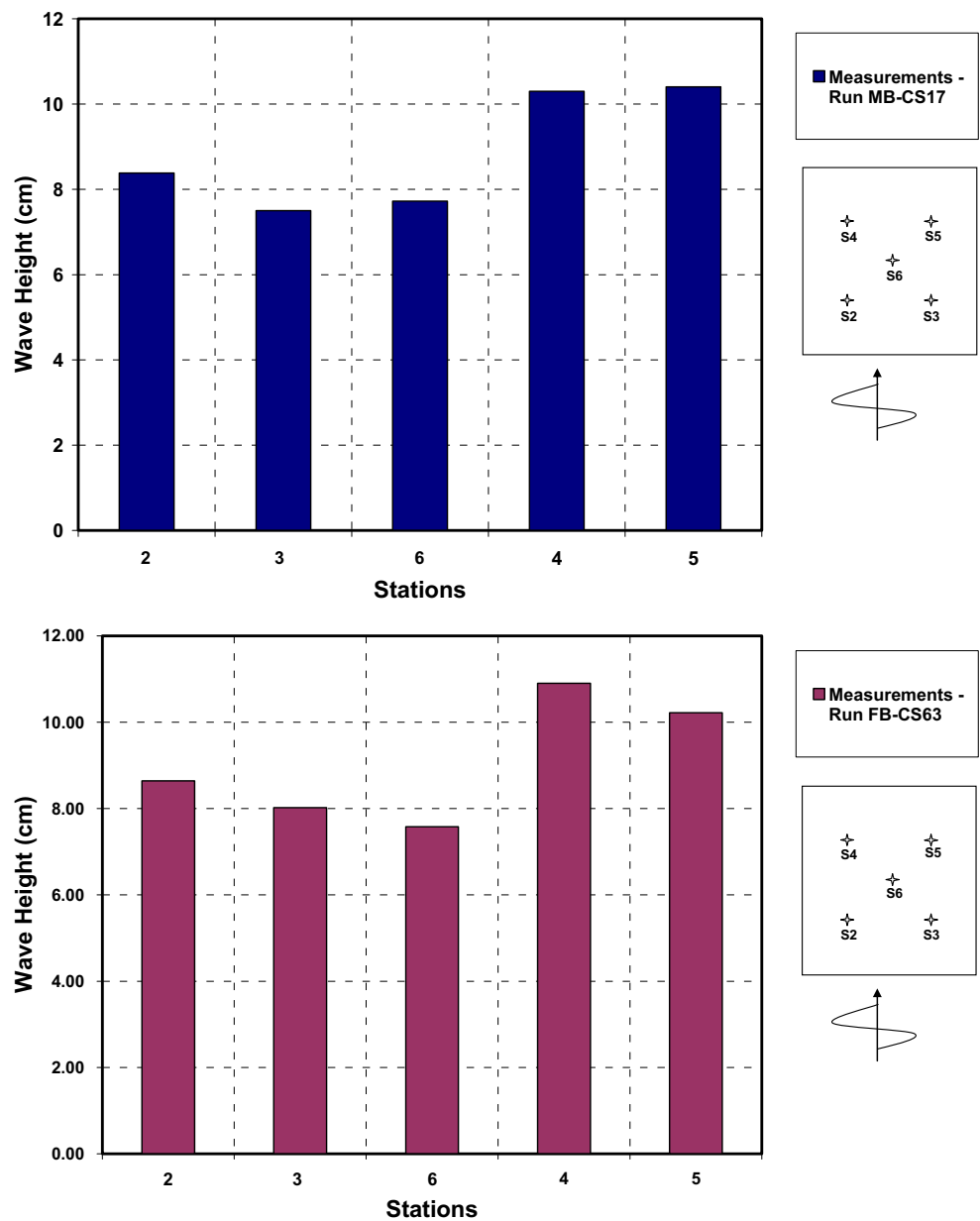
Fig. 6 Measured wave heights over the muddy bed (*up*; MB-CS18, incident wave height 7.3 cm and wave period 1.4 s) as well as the fixed bed (*down*; FB-CS64, incident wave height 7.3 cm and wave period 1.4 s)
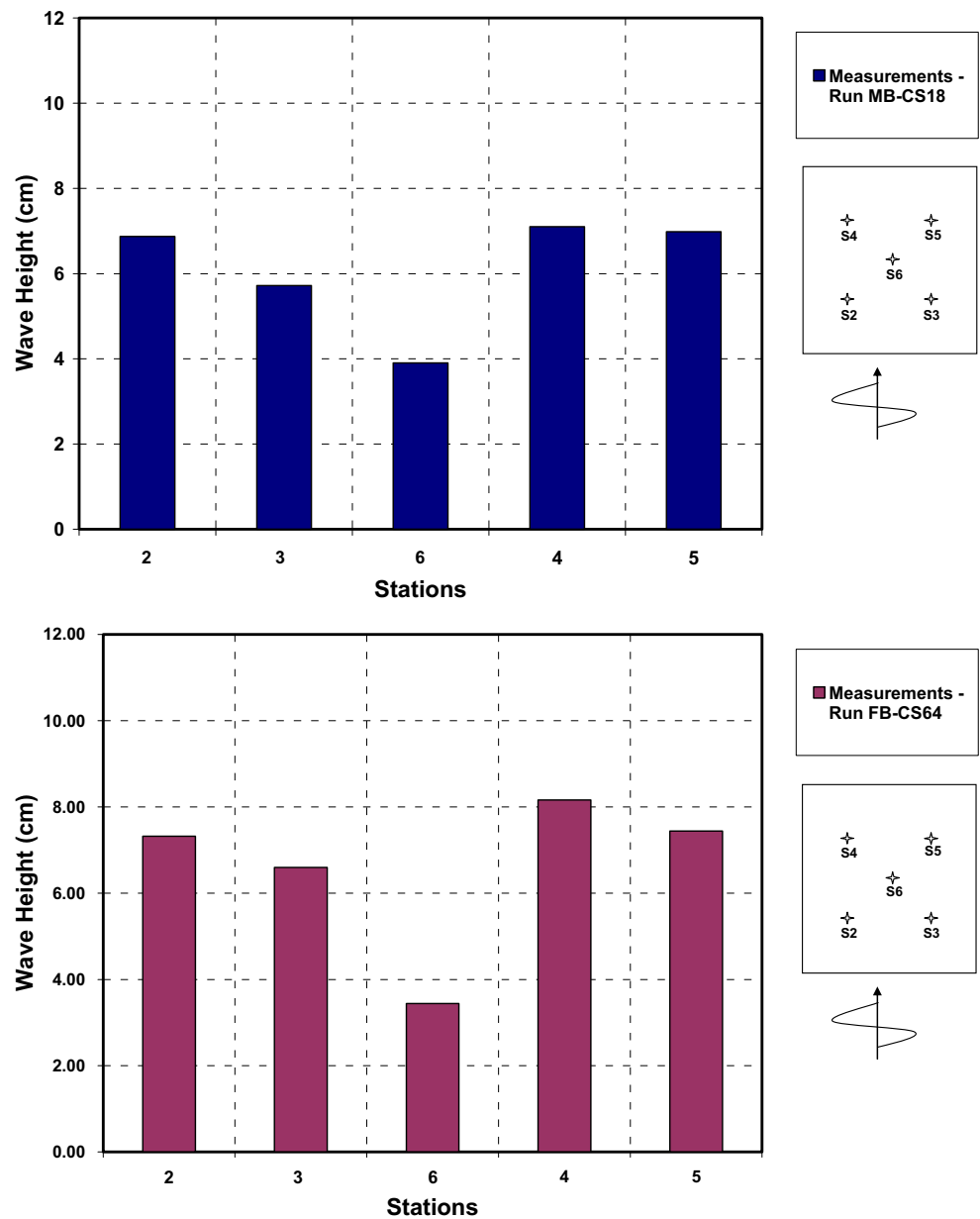
the water layer is represented by *N*=1. Figure 8 shows the definition of the multi-layered wave–mud interaction model. Different mud characteristics in each horizontal sub-layers of the fluid mud layer can be applied. The rheological equations of the viscoelastic model are used for the fluid mud behavior. The viscoelastic parameters, i.e., μ and G, are adopted by interpolating the laboratory data as presented in Table 2. The governing equations for the system of water and fluid mud layers are the linearized Navier–Stokes equations, neglecting the convective accelerations, and the continuity equation.

Five *N* boundary conditions exist for a fluid model of *N* sub-layers as presented by Maa (1986) and Tsuruya et al. (1987). The boundary conditions consist of kinematic boundary conditions, which are the continuity of horizontal and vertical velocities at interfaces and zero horizontal and vertical

velocities at the rigid bottom, and the dynamic boundary conditions, i.e., zero normal and tangential stresses at the water surface and the continuity of normal and tangential stresses across the interfaces. The wave attenuation rate, k_i, can be calculated by this model. The details of the wave–mud interaction model have been provided by Soltanpour et al. (2003).

Assuming an exponential wave height decay on a gentle muddy slope, the mud-induced energy dissipation rate, ε_{Dm}, is related to the wave attenuation rate, k_i, through the following expression (Soltanpour et al. 2003):

$$\varepsilon_{Dm} = -\frac{\partial}{\partial x}\left(C_g E\right) = 2 C_g k_i E \tag{4}$$

Consequently, the aforementioned parameter w_m, i.e., the fluid mud dissipation parameter defined as the ratio
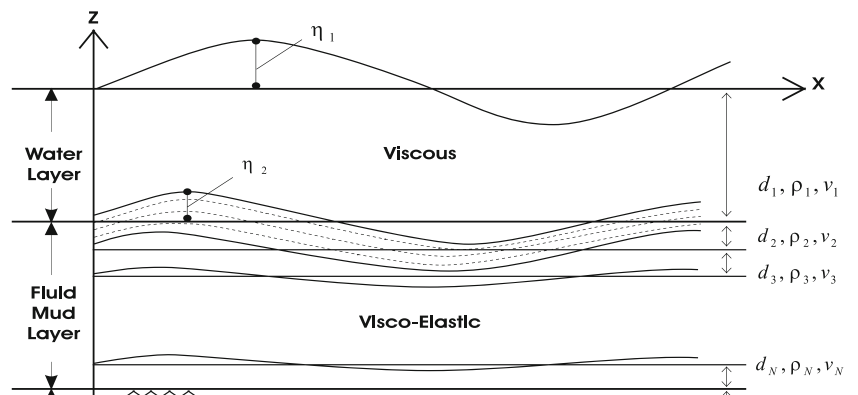
Fig. 7 Measured wave heights over the muddy bed (*up*; MB-CS19, incident wave height 3.9 cm and wave period 1.8 s) as well as the fixed bed (*down*; FB-CS66, incident wave height 3.3 cm and wave period 1.8 s)
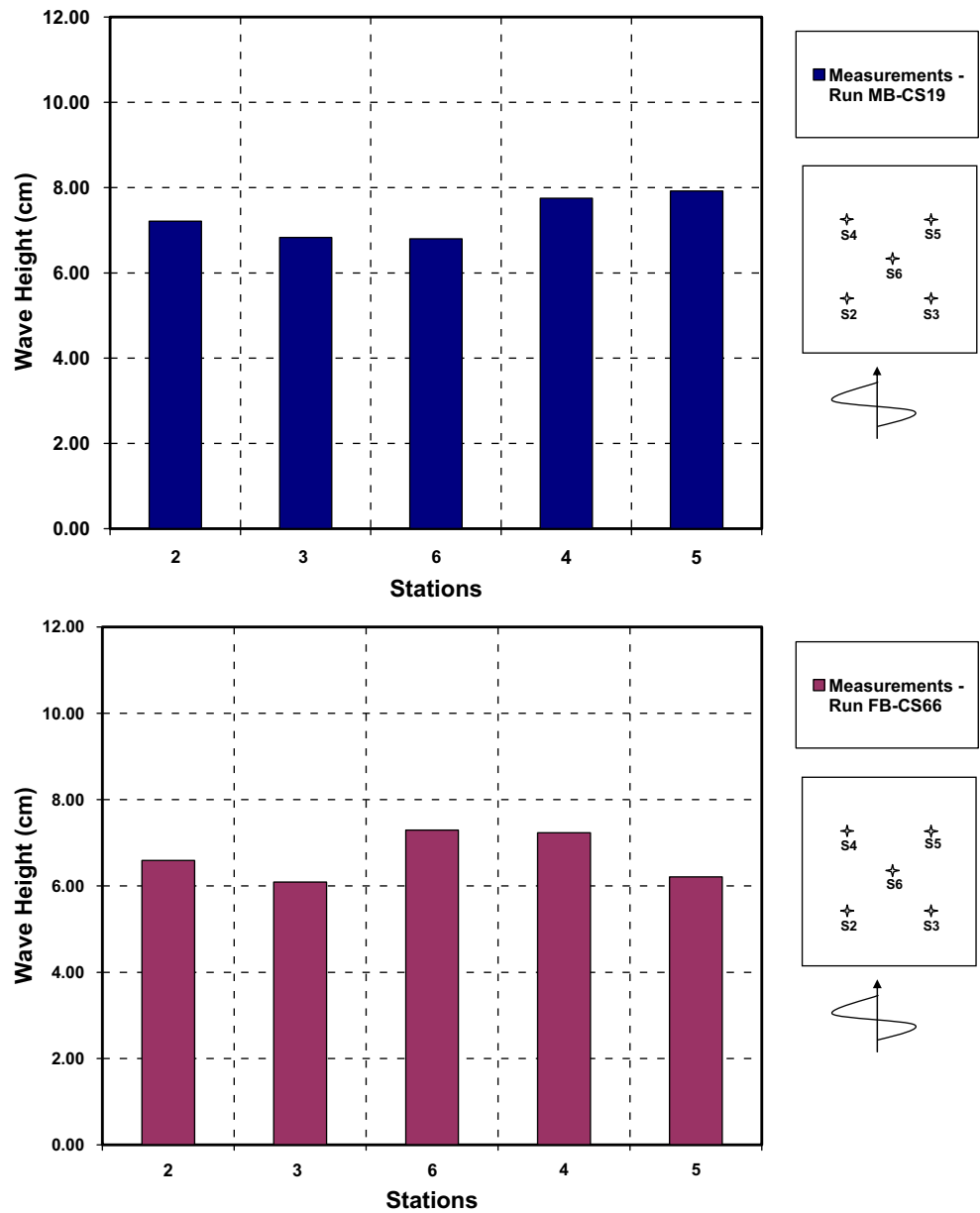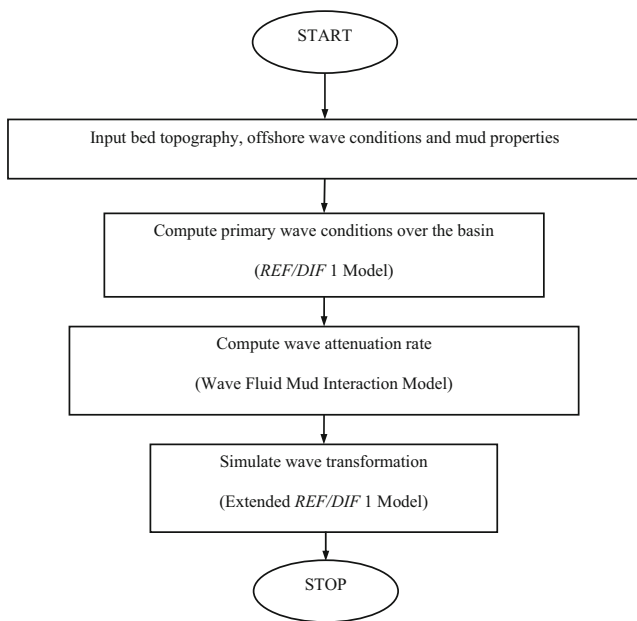

of energy dissipation and energy, can be defined as below:

$$w_m = \frac{\varepsilon_{Dm}}{E} = 2C_g k_i \qquad (5)$$

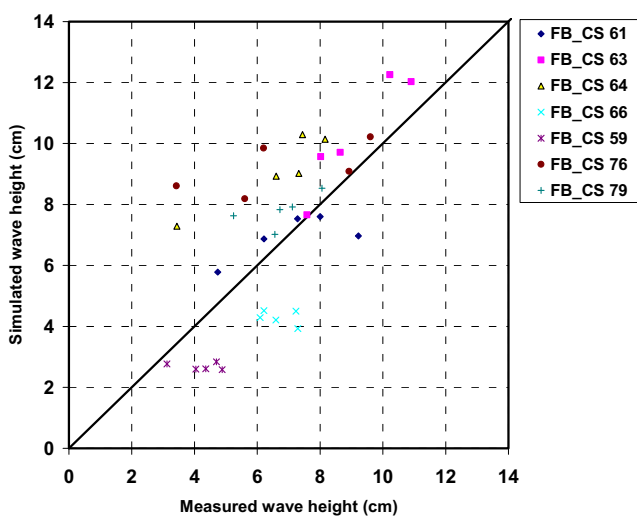**Fig. 8** Definition of multi-layered wave–mud interaction model

Fig. 9 Flowchart description of the composite wave model

Fig. 11 Comparison between measured and computed wave heights at different stations over the mud box for seven runs listed in Table 3, i.e., muddy bed runs (RMSE=1.74, SI=0.23, bias=−0.77, and CC=0.58)
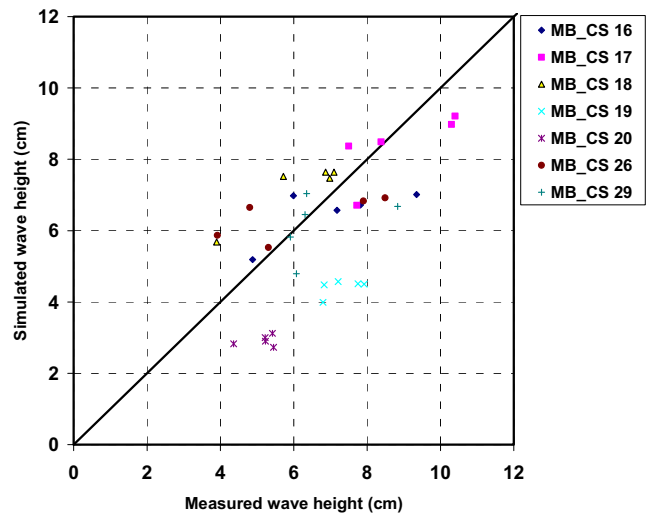
where $E=\rho g H^2/8$ is the wave energy per unit surface area and C_g is the group velocity. After breaking, the energy dissipation parameter reflects both dissipation effects of wave breaking and fluid mud, i.e.,

$$w = w_m + w_b \qquad (6)$$

The computed dissipation parameter is introduced to the REF/DIF 1 model, through an input file defining the mud-induced relative wave attenuation rate at the various grid points of the domain, to include the effects of muddy bed existence in the domain area.

4.3 Method of calculations

The described numerical model is a composite one, consisting of two major modules. The main component of the model is REF/DIF 1 wave model which does not consider wave dissipation associated by the fluid mud layer. In order to include wave–mud interaction effects, an integrated wave model is introduced with the following components:

- Wave dissipation rate is simulated using a multi-layer fluid system assuming viscoelastic rheological behavior for the fluid mud layer (wave–fluid mud interaction model).
- Wave transformation is calculated in REF/DIF 1 wave model software including muddy bed effects.

Fig. 10 Comparison between measured and computed wave heights at different stations over the box for seven fixed bed runs listed in Table 4 (RMSE=1.57, SI=0.21, bias=−0.62, and CC=0.72)
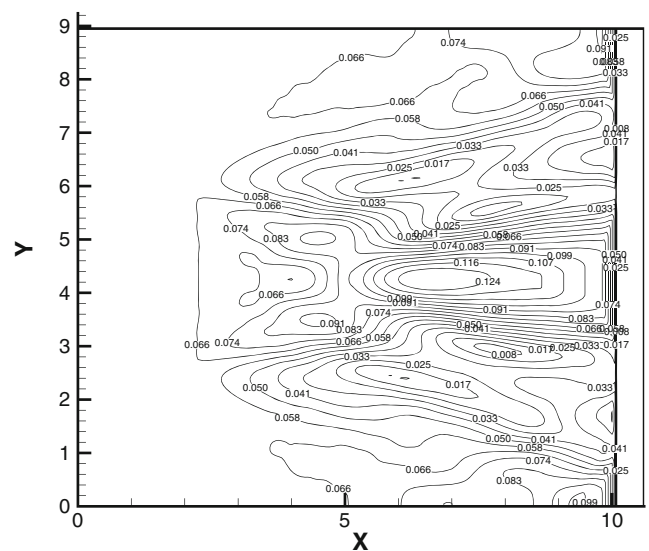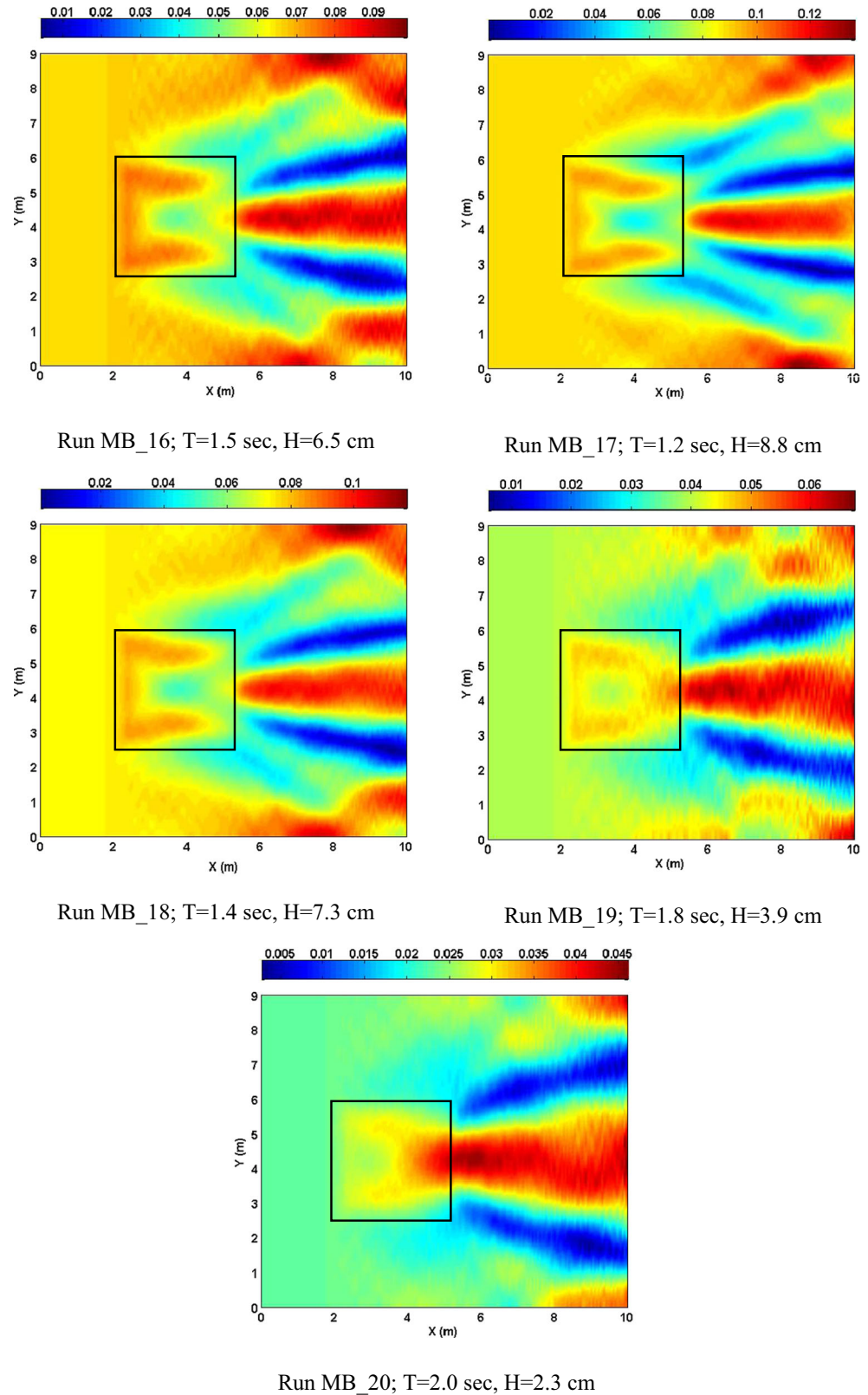

Fig. 12 Computed wave height contours by REF/DIF 1 over the basin, experimental case FB-CS63

Input data consist of necessary information describing the incident wave characteristics, bottom topography, and the fluid mud water content ratio. The incident wave characteristics,

bottom topography, and initial values of mud-induced dissipation go to the REF/DIF model to compute wave characteristics over the computation domain. The fluid mud thickness is as a

Fig. 13 Computed wave heights for five runs over the mud box, listed in Table 3; the *box* shows the location of the mud patch

Run MB_16; T=1.5 sec, H=6.5 cm

Run MB_17; T=1.2 sec, H=8.8 cm

Run MB_18; T=1.4 sec, H=7.3 cm

Run MB_19; T=1.8 sec, H=3.9 cm

Run MB_20; T=2.0 sec, H=2.3 cm

specified input parameter for the wave–fluid mud interaction model, where the wave–fluid mud interaction is applied to calculate and update the wave dissipation rate initial values, considering computed wave parameters, depth data, and fluid mud water content ratio. As the mud sampling during laboratory experiments did not show any change of concentration within the mud layer, the entire fluid mud layer was assumed as a single layer in the wave–mud

interaction module. Introducing the dissipation rate into the REF/DIF 1 model through *w* component, the wave model is used to compute the wave height at the next grid cell combining the shallow water processes and dissipation effects of fluid mud. The dispersion equation is modified by the results of multi-layered model to include mud effects on group wave celerity. Figure 9 shows the flowchart of the proposed extended REF/DIF 1 model.

Fig. 14 **a** Computed cross-sectional wave height contours for MB_CS16 run along cross-sectional lines crossing from S2–S3 to S6 and S4–S5 stations. **b** Computed cross-sectional wave height contours for FB_CS61 run along cross-sectional lines crossing from S2–S3, S6 and S4–S5 stations
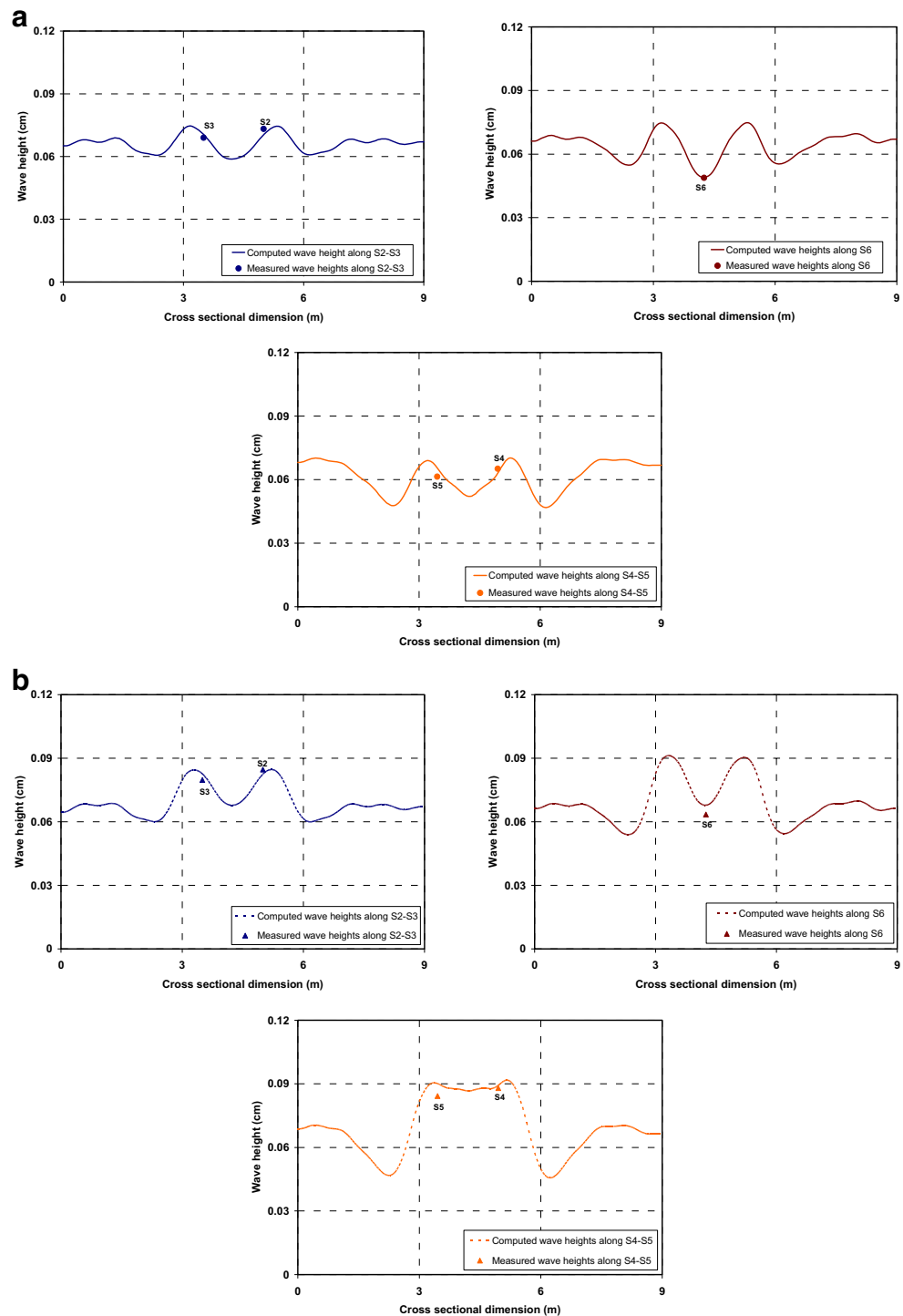
5 Model performance and discussion

5.1 Validation

The described extended REF/DIF 1 wave model can be utilized to get regular wave transformation on muddy beds. Performance of the model against recorded wave basin experimental data is examined in this section. In order to check the wave model performance, model results over the fixed bed were compared against measured wave heights for the cases listed in Table 4. A comparison between the REF/DIF 1 results and recorded wave heights for the laboratory fixed bed runs, where the box surface is covered by a fixed surface, not soft mud, is presented in Fig. 10. It is shown that the laboratory measurements are estimated with acceptable accuracies by the wave model. The figure also shows the statistical parameters of bias, root mean square error (RMSE), scatter index (SI), and correlation coefficient (CC) of the scatter wave heights. The underestimated computed wave heights at lower frequency runs might be attributed to their longer wave lengths that cause the waves not to be well developed in the basin and in the short distance between wave paddles and beginning of the box. Excluding the two lower frequency cases, computed values for the other runs are overestimated which might be attributed to the energy dissipation due to the rough surface of the fixed bed as well as energy absorption by the gravel side slopes of the box; both of which are not considered in the model.

Similarly, the computed wave heights at different stations over the mud box are compared with measurements in Fig. 11. Considering the comparisons in Fig. 11, it is concluded that output results of the extended REF/DIF 1 model are in reasonable agreements with the measurements; however, similar to the fixed bed experiments, the deficiencies of laboratory conditions (e.g., limitations of performing experiments on the slope, steep bottom slope in basins, relatively small dimensions of basins which consequently results in small dimensions of the mud layer) and numerical model (e.g., consideration of not fully nonlinear equations) are responsible for the reduction of the accuracy of predictions. The complex diffraction pattern also affects the modeling accuracies in Figs. 10 and 11.

Figure 12 presents the computed wave height contours over the model domain for case FB_CS63 of Table 4 to illustrate the complex behavior of wave transformation over the wave basin in the absence of a mud layer. It is clearly observed that bottom friction, shoaling, and wave diffraction are generating a complicated pattern of wave height distribution, particularly over the shoal, which is considerably affected by wave diffraction from the sides.

5.2 Further study of the influence of mud on the various processes

Introducing incident wave characteristics and mud rheological parameters to the extended REF/DIF 1 model, Fig. 13

illustrates the computed wave height contours over the model domain for the five experimental cases listed in Table 3. It is observed that the results of wave transformation over the box are highly affected by wave diffraction from the sides. In the experimental cases with higher frequencies, the dominant phenomenon is a combination of interacting waves with the muddy environment and wave diffraction from the sides; moreover, the area affected by the shoal gets narrower with a decrease in wave period. On the other hand, although the
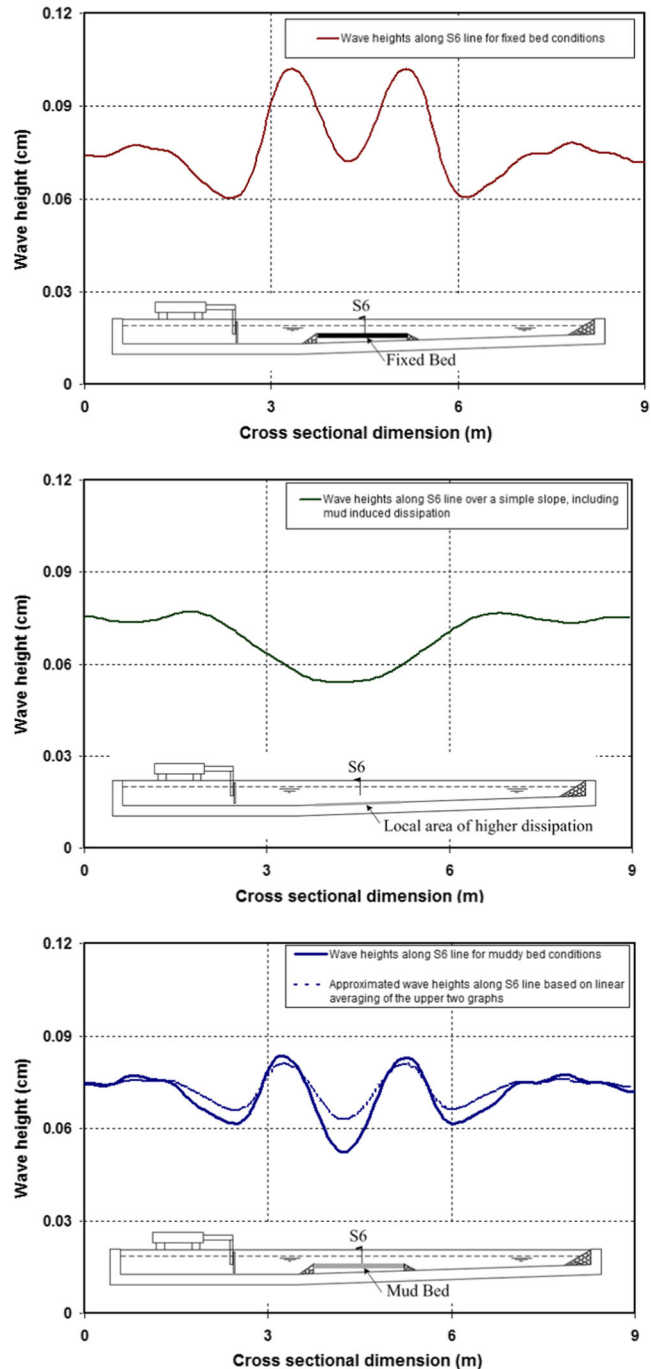

Fig. 15 Computed wave heights along S6 line for MB_CS18, with different bathymetry and bottom conditions

affected area is broader for the two cases with lower frequencies, the mentioned combination is not as effective as the cases with higher frequencies. Figure 14 presents cross-sectional wave height contours along S2–S3, S6, and S4–S5 lines over the box for selected mud bed (MB_CS16) and fixed bed (FB_CS61) cases, respectively. It is observed that the wave heights are attenuated between S2–S3 line and S4–S5 one over the muddy bed, while the wave heights increase over the fixed bed (see Fig. 14).

Moreover, the double peaks over the box area reveal wave diffraction from the sides over the mud box; similarly, local presence of relatively high energy dissipation at the bottom causes the incident wave field to diffract toward the area of higher dissipation rates. Hence, the wave transformation process over the mud box is affected by the combination of two wave diffraction phenomena, one due to the mud box and its surrounding slopes as a shoal and the other one to the higher energy dissipation area formed by the mud layer inside the box, as an imaginary shoal. In order to demonstrate the contribution of the described diffractions, Fig. 15 shows computed wave heights along the S6 line for incident wave condition of run MB_CS18 with different wave conditions. The upper frame shows wave height variations along the line considering a fixed bed all over the box, and the middle graph shows similar simulation results transformed over a simple 1:30 slope while corresponding mud-induced dissipation is included over the mud box area. The dissipation quantities are directly taken from relevant grids in the original wave transformation model for run MB_CS18. As it is seen, wave diffraction is obvious toward the region of higher energy dissipation. The bottom graph presents a comparison between computed wave heights through the extended REF/DIF 1 wave model for real conditions of run MB_CS18 (the solid line) and an average of the upper two graphs (the dashed line). The latter line represents an approximation of wave heights over S6 line by linear averaging of effective parameters. The averaged line reveals similar pattern and peaks as simulated for the real case.

In order to demonstrate the contribution of mud-induced dissipation, Fig. 16 depicts a comparison between the computed cross-sectional wave contours including and excluding mud existence. As it is observed, the computed waves over the fixed bed are larger than the similar ones on the mud bed. As the wave advances, the differences are more considerable
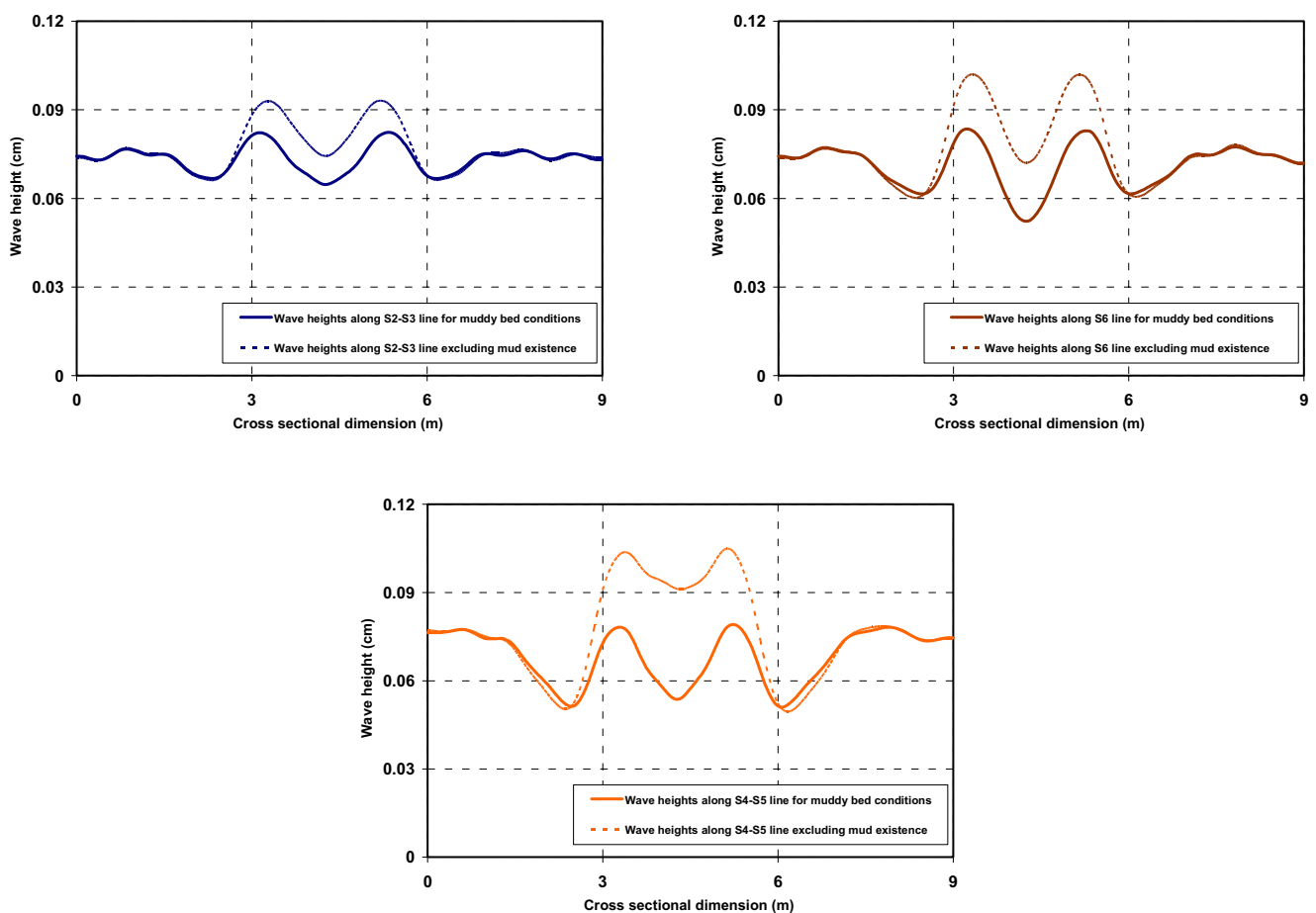
Fig. 16 Comparisons between computed wave heights at different stations over the mud box, including and excluding the mud-induced wave dissipation

Fig. 17 Computed wave heights for two cases from Table 3 with obliquely incident waves; the *box* shows the location of the mud patch

Run MB_26; T=1.4 sec, H=6.5 cm   Run MB_29; T=1.2 sec, H=7.0 cm
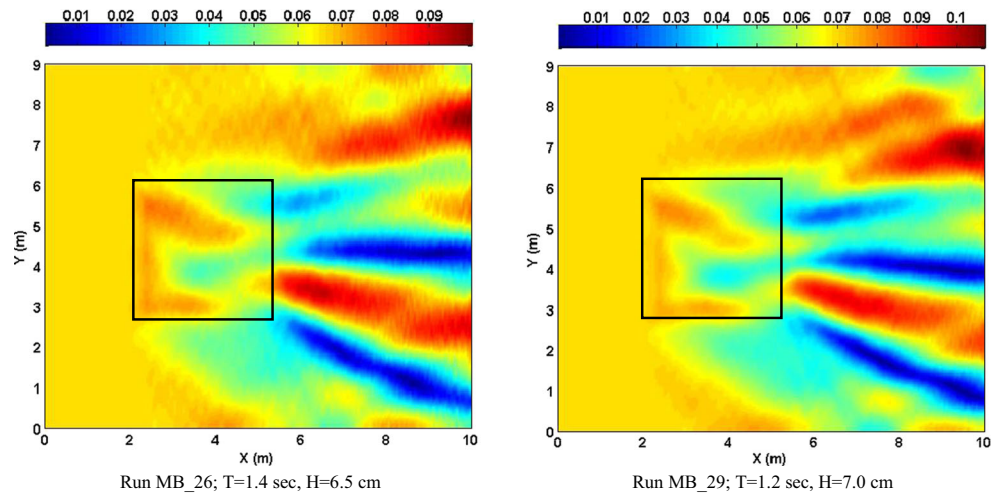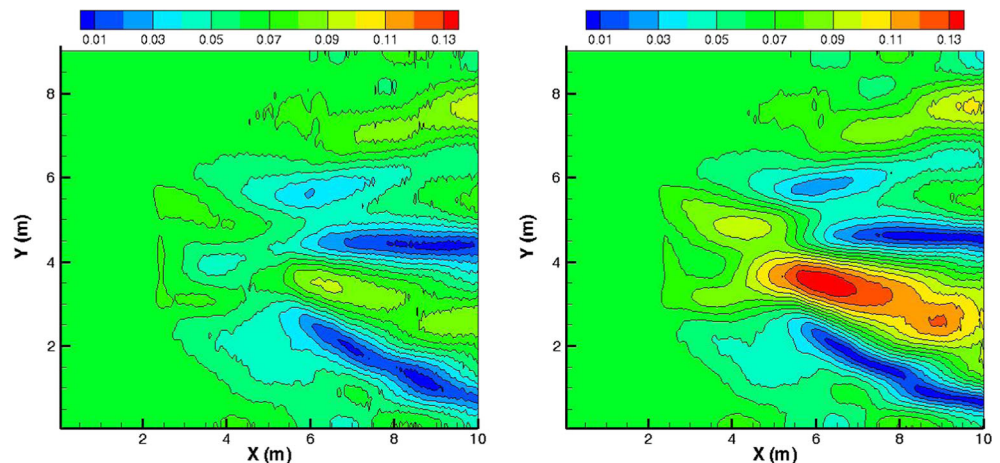
which reveals that the mud-induced dissipation is effectively contributing to the wave propagation.

5.3 Obliquely incident waves

In the last two cases of Table 3, with obliquely incident waves, wave refraction is more emphasized. The strong wave attenuation through the mud patch and the shadow zone in the lee of the patch are still observed (Fig. 17). The whole pattern of wave height distribution is not asymmetric as expected; however, the asymmetries over the box are more highlighted, where the darker shade on the box, which represents larger wave heights, are more deviated at the upper zone of larger waves due to the effects of incoming oblique waves interacting with the ones over the box comparing with the lower zone of larger wave heights where the surrounding outer waves are getting far from the area. On the other hand, Fig. 18 illustrates diffraction patterns for case MB_26 including and excluding mud-induced dissipation. It is revealed that although the mud considerably absorbs the wave energy, no significant change is observed in the diffraction patterns.

6 Summary and conclusion

The present study can be summarized as follows:

1. A set of wave basin experiments was performed to investigate two-dimensional wave transformation over muddy beds. Similar tests were also conducted on a fixed bed in order to provide comparable data in the absence of a mud layer.
2. The wave transformation on the mud box shows a complicated pattern which is a combination of energy absorption by the muddy bed and wave transformation features of shoaling and diffraction. The combination of wave height attenuation with other shallow water processes results in a compound wave field over the mud layer which is not easy to elaborate.
3. An extended version of the REF/DIF 1 wave model including dissipation effects over a mud bed was employed as a coupled wave transformation model, in order to simulate the complex two-dimensional wave–fluid mud interaction. The model has the ability to simulate mud-induced wave energy dissipation to shallow water processes.

Fig. 18 Computed wave height contours for case MB_26, including (*left*) and excluding (*right*) mud-induced dissipation

4. The extended REF/DIF 1 wave model was applied to simulate the wave basin experiments. The computed results are in acceptable agreement with measured wave data.

5. Although the limited size of the mud box affects the laboratory results, the wave dissipation over the box is obvious. This leads to more energy transfer from the sides over the box.

References

Dally WR, Dean RG, Darlymple RA (1985) Wave height variation across beaches of arbitrary profile. J Geophys Res 90(C6):11917–11927

Dalrymple RA, Liu PL-F (1978) Waves over muds, a two-layer fluid model. J Phys Oceanogr 8:1121–1131

Dalrymple RA, Kirby JT, Hwang PA (1984) Waves diffraction due to areas of energy dissipation. J Waterw Port Coast Ocean Eng ASCE 110:67–79

de Boer GJ, van Dongeren AR, Winterwerp JC (2009) Wave damping by fluid mud, Research Report No. Z4700/ 1200266.007, Deltares, 34p

De Wit PJ (1995) Liquefaction of cohesive sediment by waves. *PhD dissertation*, Delft University of Technology, The Netherlands

Gade HG (1958) Effects of a non-rigid, impermeable bottom on plane surface waves in shallow water. J Mar Res 156(2):61–82

Goda Y (2000) Random seas and design of maritime structures. World Scientific Publishing Co., p 443

Hsu WY, Hwung HH, Hsu TJ, Torres-Freyermuth A, Yang RY (2013) An experimental and numerical investigation on wave-mud interactions. J Geophys Res Oceans, 118, doi: 10.1002/jgrc.20103

Isobe MTN, Huynh, Watanabe A (1992) A study on mud mass transport under waves based on an empirical rheology model. Proc. 23rd Intl. Conf. Coastal Engnrg., Venice, 3093–3106

Jain M, Mehta AJ (2009) Role of basic rheological models in determination of wave attenuation over muddy seabeds. Cont Shelf Res 29(3):642–651

Kaihatu JM, Sheremet A, Holland KT (2007) A model for the propagation of nonlinear surface waves over viscous muds. Coast Eng 54(10):752–764

Kirby JT, Dalrymple RA (1983) A parabolic equation for the combined refraction-diffraction of Stokes waves by mildly varying topography. J Fluid Mech 136:543–566

Kirby JT, Dalrymple RA (1986) Modeling waves in surf zones and around islands. J Waterw Port Coast Ocean Eng ASCE 112:78–93

Kranenburg WM, Winterwerp JC, de Boer GJ, Cornelisse JM, Zijlema M (2011) SWAN-mud, an engineering model for mud-induced wave-damping. J Hydraul Eng. doi:10.1061/(ASCE)HY.1943-7900. 0000370

Maa P-Y (1986) Erosion of soft mud by waves. Ph.D. dissertation, University of Florida, Gainesville, FL. 32611, 276p

Maa JP-Y, Mehta AJ (1988) Soft mud properties. J Waterw Port Coast Ocean Eng 114(6):765–769

MacPherson H (1980) The attenuation of water waves over a non-rigid bed. J Fluid Mech 97(4):721–742

Mei CC, Liu K-F (1987) A Bingham-plastic model for a muddy seabed under long waves. J Geophys Res 92(C13):14581–14594

Ng CO (2000) Water waves over a muddy bed: a two-layer Stokes' boundary layer model. Coast Eng 40(3):221–242

Rodriguez HN, Mehta AJ (2001) Modelling of muddy coast response to waves. J Coast Res SI21:132–148

Ross MA, Mehta AJ (1990) Fluidization of soft estuarine mud by waves. In: Bennett RH (ed) The microstructure of fine grained sediments: from mud to shale. Springer, New York, pp 185–191

Sakakiyama T, Bijker EW (1989) Mass transport velocity in mud layer due to progressive waves. J Waterw Port Coast Ocean Eng ASCE 115(5):614–633

Samsami F, Soltanpour M (2011) Transformation of wave spectra on muddy beds. 11th International Conference on Cohesive Sediment Transport, INTERCOH11, Shanghai, China, book of abstracts, pp. 195–196

Shen D (1993) Study on mud mass transport and topography change of muddy bottom due to waves, *Ph.D. dissertation*, The University of Tokyo, 167 p

Sheremet A, Stone GW (2003) Observations of nearshore wave dissipation over mud sea beds. J Geophys Res 108(C11):3357. doi:10. 1029/2003JC001885

Sheremet A, Mehta AJ, Liu B, Stone GW (2005) Wave-sediment interaction on muddy inner shelf during Hurricane Claudette. Estuar Coast Shelf Sci 63:225–233

Shibayama T, An NN (1993) A visco-elastic-plastic model for wave-mud interaction. Coast Eng Jpn 36(1):67–89

Soltanpour M, Shibayama T, Noma T (2003) Cross-shore mud transport and beach deformation model. Coast Eng J 45(3):363–387

Soltanpour M, Oveisy A, Shibayama T (2008) Numerical modeling of wave transformation on muddy coasts. Coast Eng J JSCE 50(2): 143–160

Tsuruya H, Nakano S, Takahama J (1987) Interaction between surface waves and a multi-layered mud bed. Rep Port Harbor Res Inst Minist Transp Jpn 26(5):138–173

Wells JT, Kemp GP (1986) Interaction of surface waves and cohesive sediments: field observations and geologic significance. In: Mehta AJ (ed) Estuarine cohesive sediment dynamics. Springer, New York, pp 43–65

Winterwerp JC, de Graaff RF, Groeneweg J, Luyendijk AP (2007) Modelling of wave damping at Guyana mud coast. Coast Eng 54: 249–261